Letter

Anomalously small superconducting gap in a strong spin-orbit coupled superconductor: β-tungsten

Prashant Chauhan,[1,*] Ramesh Budhani,[2] and N. P. Armitage[1,†]
[1]*Department of Physics and Astronomy, The Johns Hopkins University, Baltimore, Maryland 21218, USA*
[2]*Department of Physics, Morgan State University, Baltimore, Maryland 21251, USA*

(Received 6 October 2021; revised 28 January 2022; accepted 14 February 2022; published 22 February 2022)

Thin films of β-tungsten host superconductivity in the presence of strong spin-orbit coupling. This nonequilibrium crystalline phase of tungsten has attracted considerable attention in recent years due to its giant spin Hall effect and the potential promise of exotic superconductivity. However, more than 60 years after its discovery, superconductivity in this material is still not well understood. Using time-domain terahertz spectroscopy, we measure the frequency response of the complex optical conductivity of β-tungsten thin film with a T_c of 3.7 K in its superconducting state. At temperatures down to 1.6 K, we find that both the superconducting gap and the superfluid spectral weight are much smaller than that expected for a weakly coupled superconductor given the T_c. The conclusion of a small gap holds up even when accounting for possible inhomogeneities in the system, which could come from other crystalline forms of tungsten (that are not superconducting at these temperatures) or surface states on β tungsten grains. Using detailed x-ray diffraction measurements, we preclude the possibility of significant amounts of other tungsten allotropes, suggesting the topological surface states of β-tungsten could play the role of inhomogeneity in these films. Our observations pose a challenge and opportunity for a theory of strongly anisotropic normal metals with strong spin-orbit coupling to be described.

DOI: 10.1103/PhysRevB.105.L060503

Bulk crystalline tungsten (W) in the most stable α-W bcc form has a very low superconducting T_c of 11 mK [1]. However, thin films of W can have T_c's as large as 5 K, e.g., two orders of magnitude higher than the bulk. This has been attributed to the presence of a metastable A15 β phase structure that can be stabilized in thin films [2,3]. Such β-W has very distinctive mechanical, electrical, and optical properties. Its room temperature resistivity ($\sim$200 $\mu\Omega$ cm) is much higher than that of α-W ($\sim$20 $\mu\Omega$ cm) [4]. Due to strong spin-orbit coupling (SOC), β-W exhibits a giant spin Hall effect with large spin Hall angle ($\theta_{SH} \sim -0.45$), making it potentially useful in spintronic applications [5,6]. Density functional theory calculations show that β-W may be a Dirac system that hosts massive Dirac fermions and may host surface arc states with novel spin textures reminiscent of those in topological insulators [7,8]. The helical spin-polarized electrons in topological insulators can host exotic excitations like Majorana fermions if their topological surface states become superconducting by proximity effect [9]. These facts prompt us to investigate the possibility of exotic bulk and surface superconductivity in β-W.

The study of superconductivity in β-W thin films has proven to be challenging. There have been only a few experimental and theoretical investigations [1,2,10] that have given an understanding of its superconducting state and order parameter. This is mainly because of the difficulty in growing clean β-W thin films without impurity phases like α-W and the instability of this metastable phase at room temperature where it can spontaneously transform into the α-W phase [11]. However, there has been a long-term (and now renewed) interest in both the metallic state and the superconductivity of β-W. The superconductivity exhibits a number of unusual aspects. Using tunneling, Basavaiah and Pollack showed that the temperature dependence of the superconducting energy gap $\Delta(T)$ follows the Bardeen-Cooper-Schrieffer (BCS) dependence [2], but with a reduced ratio $\alpha = \Delta/k_B T_c \sim 1.1$–$1.8$ (where Δ is the superconducting energy gap) as opposed to the universal weak-coupling BCS value of $\alpha_{BCS} \sim 1.76$ [2,12]. It was suggested that the reduced gap could be related to the presence of the α-W phase [2]. We shall revisit this possibility below.

In general, the $\alpha = \Delta/k_B T_c$ ratio provides important insight into the physics. In a clean system, the coupling strength of superconductivity can be defined relative to α_{BCS}, with $\alpha \simeq \alpha_{BCS}$ for a weakly coupled superconductor and α somewhat greater than α_{BCS} for a strongly coupled superconductor. In disordered systems, pair breaking tends to decrease T_c faster than it does the Δ, which increases the ratio above α_{BCS} [13]. Thus, in general we expect $\alpha \geqslant \alpha_{BCS}$ [13], which is in contrast to observations in β-W [2]. However, in such considerations, there is an implicit assumption that the order parameter is uniform both in space and in momentum. The order parameter can be anisotropic in momentum space and the gap on the Fermi surface $\langle\alpha\rangle$ can be at points smaller than α_{BCS} [13]. Due to a complicated and nonuniform Fermi surface [7], we expect β-W to possess an anisotropic superconducting gap [14]. However, the question is to what degree? Real space inhomogeneity can of course create regions where the gap is suppressed and this may also be an effect.

*pchauha1@jhu.edu
†npa@jhu.edu

Here we use high precision time-domain terahertz (THz) spectroscopy (TDTS) to measure the low-energy complex optical conductivity of β-tungsten films as a function of temperature. We systematically study and track the superconducting gap, $\Delta(T)$, as a function of temperature. We find that the superconducting energy gap and the superfluid density can be described phenomenologically in terms of BCS theory, however, with a small energy gap parameter. This confirms a value of α much smaller than the 1.76 than expected for a weakly coupled BCS superconductor. The conclusion of a small gap holds up even when using extant effective medium models that account for inhomogeneity in the form of normal metal inclusions. Such inclusions could come from other crystalline forms of tungsten (not superconducting at these temperatures) or surface states on β-tungsten grains. Our observations pose a challenge and opportunity for a theory of strongly anisotropic normal metals with strong spin-orbit coupling to be described.

Thin films of the β-tungsten (A15 structure) were grown on 0.5-mm thin Si(001) with ~200-nm-thick thermal oxide and 0.5 mm MgO(100) substrates using sputtering in the presence of N_2:Ar gas mixture at room temperature. The Ar sputtering pressure was kept at 5 mTorr during the deposition. The fact that β-W thin films require N_2:Ar or O_2:Ar mixture assisted growth has made it difficult to tune the quality and T_c of the superconducting film. TDTS measurements were performed in transmission geometry on thin films of varying thicknesses ranging from 70 to 130 nm. The 70-nm β-W thin films had the highest T_c's of ~3.7 K. The samples on both Si and MgO substrates gave similar results [see Supplemental Material [15] (SM)]. Both real and imaginary parts of the complex conductance, $\tilde{G}(\nu)$, were extracted from the complex transmission measured in TDTS measurements, performed down to 1.6 K [21].

Figure 1 shows the frequency dependent transmission and complex conductivity $\tilde{G}(\nu)$ of a 70 nm β-W film, between 0.2 and 1.6 THz in zero magnetic field at a few different temperatures above and below T_c. For $T > T_c$, the real part of the conductance, $G_1(\nu)$, is constant in both this frequency and temperature range with RRR ~ 1. In the normal state, $G_2(\nu)$ is zero in correspondence with the large scattering rate ($\gg$10 THz). The THz conductance in the normal state 0.03 Ω^{-1} matches well with dc conductance measurement, $G_{dc} =$ 0.028 Ω^{-1}. Below T_c both $G_1(\nu)$ and $G_2(\nu)$ show features indicative of the opening of a superconducting energy gap. As the temperature falls below T_c, a depletion develops in $G_1(\nu)$ at low ν, corresponding to the shift of the superconducting carrier spectral weight to the zero frequency delta function [22]. However, the depletion is not large and even at the lowest temperatures of 1.6 K, the conductance remains ~66% of the normal state at 0.2 THz. For a weak-coupling BCS superconductor with $T_c \sim 3.7$ K, one expects an optical 2Δ gap of about 0.27 THz at this temperature. $G_1(\nu)$ shows a small upturn below 0.2 THz. As $\nu \to 0$, $G_2(\nu)$ shows $1/\nu$-like dependence at the lowest temperatures, characteristic of the superconducting state.

To understand the superconducting state better and determine the energy gap $\Delta(T)$, we simultaneously fit the normalized $G_1(\nu)$ for *all* temperatures to the Mattis-Bardeen (MB) theory [21,23,24]. Normalizing the low temperature

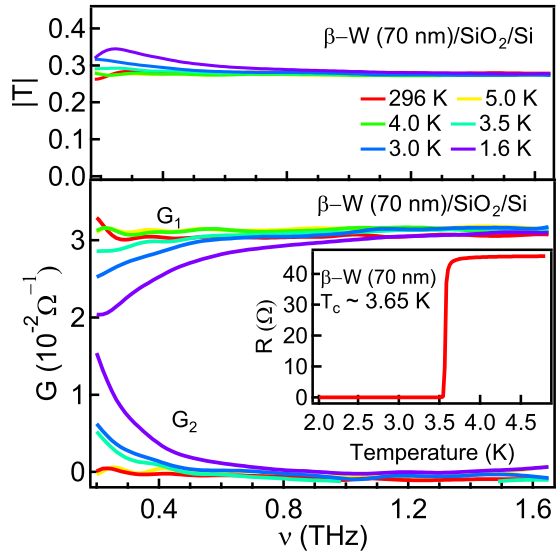

FIG. 1. Top: Zero-field magnitude of transmission. Bottom: Real $G_1(\nu)$ and imaginary $G_2(\nu)$ parts of the zero-field complex conductance of β-W 70-nm thin film grown on Si substrate as a function of frequency from room temperature ($T \gg T_c$) to (1.6 K $\ll T_c$). Inset: Temperature dependence of the four-probe dc resistance.

conductance with the normal-state conductance, $G_1(5\text{ K})$ eliminates a number of the systematic errors in the transmission data and reduces the number of fitting parameters. For the fitting procedure, the only free parameter is the zero temperature superconducting gap, $\Delta(0)$. The result of the fits as well as the normalized conductance data are shown as dashed and solid lines in Fig. 2. The upturn in $G_1(\nu)$ at 0.2 THz becomes more apparent after normalizing the data. The global fit to the real part of the normalized conductance for all temperatures gives $\Delta(0) = 0.32$ meV, which is similar to values obtained from tunneling spectroscopy (0.31–0.52 meV for films with T_c ranging from 3.1 to 3.3 K) [2]. There is close agreement between the MB fits and $G_1(\nu)$. In contrast, the correspondence with the imaginary part using the same parameters as the real part gives poor agreement at low frequencies (Fig. 2). Nevertheless, the temperature evolution of the superconducting gap $\Delta(T)$ follows standard BCS $\Delta(T) = \Delta(0)\tanh[1.74\sqrt{T_c/T-1}]$, given for a weakly coupled BCS superconductor. However the extracted gap $2\Delta(0) = 0.15$ THz (0.64 meV) or $\alpha = \Delta(0)/k_B T_c \sim 1$ is much less than the weak-coupling limit of 1.76 for a fully gapped BCS superconductor.

To get further insight into the superconducting gap and confirm the Mattis-Bardeen fits, we study the temperature dependence of the superfluid spectral weight, $S_\delta(T)$, as a measure of superfluid density n_s. We calculate $S_{\delta,G_2} = \lim_{\nu\to 0}\nu G_2/G_n$ which is a measure of superfluid spectral weight determined directly from the TDTS experimental data. We can compare it to the value calculated $S_{\delta,\text{MB}}$ for $\alpha = 1$ and $\alpha_{\text{BCS}} = 1.76$ using the approximation for a fully gapped BCS superconductor given by $S_\delta(T) = \frac{S_\delta(0)\Delta(T)}{\Delta(0)}\tanh[\Delta(T)/2k_B T]$ [24]. The normalization constant $S_\delta(0)$ is given by the Ferrell-Glover-Tinkham (FGT) sum rule, $S_\delta(0) = S_n - S_{qp}(0)$, where S_n is the total spectral weight in normal state and $S_{qp}(0)$ is the

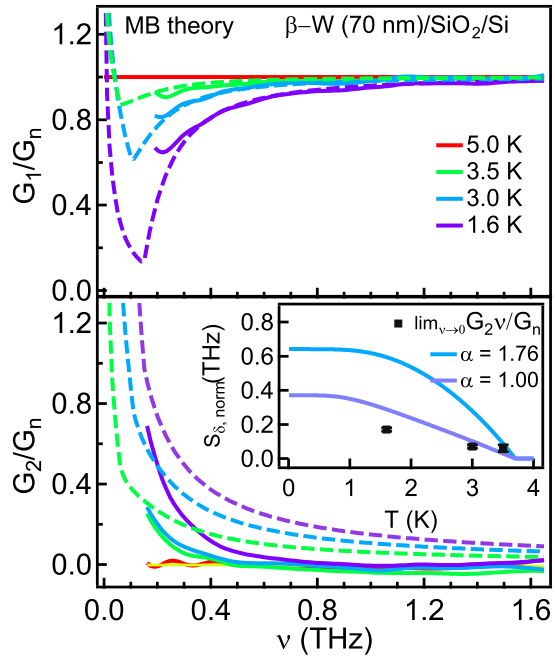

FIG. 2. Real $G_1(\nu)$ and imaginary $G_2(\nu)$ parts of the zero-field complex conductance of β-W 70-nm thin film, normalized to the normal-state conductance G_n. The solid lines are experimental data normalized with respect to the conductance at 5 K. The dashed lines are fit to the data using the Mattis-Bardeen theory for the BCS superconductor. Inset: Black squares show the temperature dependence of the superfluid spectral weight $S_\delta(T)$ determined from $\lim_{\nu\to 0}\nu G_2/G_n$. The blue line shows the expected spectral weight for a weakly coupled BCS superconductor ($\alpha_{BCS} = 1.76$). The purple line shows the expected spectral weight for a BCS-like superconductor but with the experimentally determined $\Delta(0) = 0.32$ meV that gives $\alpha = 1$.

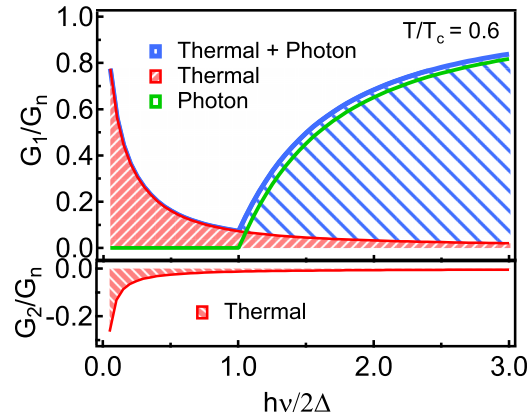

FIG. 3. Frequency dependent real $G_1(\nu)$ and imaginary $G_2(\nu)$ conductance of a superconductor at $T/T_c = 0.6$. The red shaded region indicates the thermally excited contribution. In $G_1(\nu)$, the green line indicates the photon excited response and the blue shaded region corresponds to the total response. In addition to these contributions there is a zero frequency delta function in G_1 and its very large $1/\nu$ contribution to G_2.

above gap spectral weight at $T \sim 0$ as given by the MB theory [21]. In Fig. 2 (inset) we compare the temperature evolution of S_{δ,G_2} with both $S_{\delta,\mathrm{MB}}$ for $\alpha = 1$ and $\alpha_{\mathrm{BCS}} = 1.76$. Near T_c, the curve for $\alpha = 1$ is close to the experimental value, but overestimates the spectral weight found in the delta function. Thus we conclude that the Mattis-Bardeen fits below 0.2 THz do not match the actual conductance $G_1(\nu)$ and $S_{\delta,\mathrm{MB}}(T)$ at low temperatures. It is likely that there is a subgap conductance coming from a contribution other than the ones considered in the MB theory. Hence, as compared to a weakly coupled BCS superconductor, β-W has a much lower superfluid density.

In order to qualitatively understand the origin of the low superfluid spectral weight in comparison to the MB theory prediction, we compare the experimental data phenomenologically with the individual components of the MB response function [23,25,26]. There are both thermally and photon excited contributions to the total optical response in superconductors as shown in Fig. 3. Within the BCS framework, the low-energy response of $G_1(\nu < 2\Delta)$ is only from the thermal excitations, whereas the higher-energy response above 2Δ is dominated by the photoexcitations (breaking of Cooper pairs due to photon absorption). For $G_2(\nu)$, most of the response in our spectral range is from the superfluid with a small negative contribution coming from the thermal and photon excitations, which decrease with increasing energy. On comparing the measured conductance of β-W in Fig. 2 with the individual components contributing to the optical response shown in Fig. 3, we find that the negative thermal contribution to $G_2(\nu)$ cannot account for the smaller than expected $G_2(\nu)$. It is both too small in magnitude and of course disappears in the limit of low temperature. It appears that there must be some residual low frequency metal-like conduction that has the effect of giving a smaller contribution to the lowest frequency $G_2(\nu)$ than the same spectral weight in the superconducting delta function would.

One explanation for this low n_s, a larger than expected response in $G_1(\nu)$, smaller fitted gap, and anomalous subgap absorption could be that the superconductor is inhomogeneous and that there are parts of the film which are not superconducting even at the lowest measured temperature. This would have the effect of making the apparent $\Delta/k_{\mathrm{B}}T_c$ ratio from the MB fits smaller than 1.76. Such inhomogeneity could stem from the presence of α-W, which only becomes superconducting at much lower T. α-W can either form directly during deposition or transform from β-W due to its unstable nature [2,11]. Another and surely more exciting possibility is the presence of topological surface states on the exterior of β-W grains, which could act as sources of dissipation even when the bulk of the grains becomes superconducting [7]. In order to confirm the presence of inhomogeneity, we analyze the system in terms of effective medium models. We compare the conductivity with calculations based on two different effective medium models, namely, the Bruggeman-effective-medium approximation (BEMA) [27] and the Maxwell-Garnett theory (MGT) [16], for the collective response of a mixture of two materials [17,21,28]. See SM [15] for details of these models. The BEMA treats all constituents equivalently, and is thus appropriate for mixtures with connected grains. In contrast, the

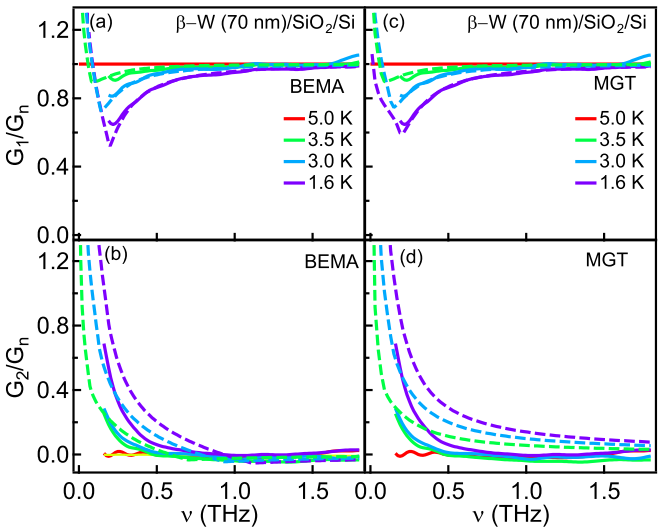

FIG. 4. Zero-field normalized real $G_1(\nu)$ and imaginary $G_2(\nu)$ conductance of 70 nm β-W thin film shown with solid lines. (a),(b) Effective optical conductance calculated from BEMA (dashed lines) with normal volume fraction $f = 0.3$. (c),(d) Effective optical conductance calculated from MGT (dashed lines) with normal volume fraction $f = 0.3$.

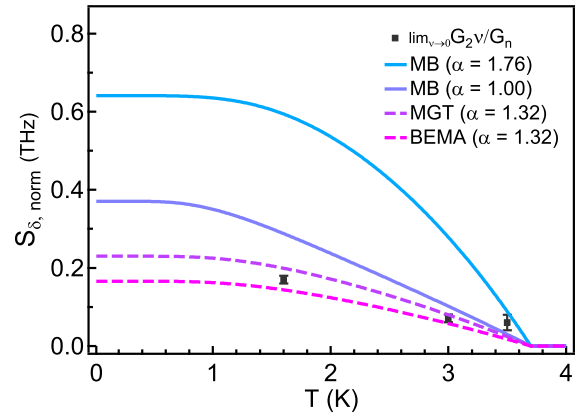

FIG. 5. Temperature dependent superfluid spectral weight, $S_\delta(T)$. The black squares show $\lim_{\nu\to 0}\nu G_2/G_n$. Solid lines are superfluid spectral weight calculated for the MB theory for $\alpha = 1$ and 1.76. Dashed lines are the superfluid spectral weights calculated for the MGT and BEMA for a normal volume fraction of $f = 0.3$.

MGT treats one constituent as the host and others as embedded media making it more suitable for mixtures with isolated inclusions [17].

For the BEMA model, we consider an inhomogeneous two component medium of normal Drude metal and superconductor that have volume fractions f and $1 - f$. Similar to the analysis above, we fit the normalized $\tilde{G}(\nu)$ using the MB theory for the superconducting fraction and the normalized $G_n(\nu) = 1$ for the normal fraction. Here the free parameters are f and $\Delta(0)$. We obtain reasonable fits for $G_1(\nu)$ with a slightly larger energy gap than in the MB homogeneous case of $\Delta(0) = 0.42(2)$ meV (0.10 THz) and normal volume fraction $f = 0.30(3)$ as shown in Figs. 4(a) and 4(b). The spectral gap $2\Delta(0)$ fit in this fashion increases only by 33% giving $\alpha_{\text{BEMA}} = 1.32$ which is somewhat closer to, but still less than the weakly coupled BCS superconductor value of 1.76. The BEMA fits for $G_2(\nu)$ match even better to the data as compared to MB theory fits in Fig. 2(b). Although there are still discrepancies, they appear to be converging towards the data at frequencies below 0.2 THz. In order to confirm the fits we determine the superfluid spectral weights of $G_1(\nu)$ from BEMA $S_{\delta,\text{BEMA}}$ using the FGT sum rule and compare it to $S_{\delta,G_2}(T)$ in Fig. 5. Unlike the overestimated superfluid spectral weights obtained from the MB theory, $S_{\delta,\text{BEMA}}$ falls only slightly below the BCS prediction and S_{δ,G_2}.

For the MGT model the superconducting component is taken as the host medium and the normal volume fraction f is taken as the embedded media. We fit $\tilde{G}(\nu)$ using the MB theory for the superconducting medium, taking the energy gap $\Delta(0)$ and normal volume fraction f as the only free parameters. Figures 4(c) and 4(d) showthat the MGT fits are consistent with $G_1(\nu)$ for $f = 0.3$ and energy gap $\Delta(0) = 0.42$ meV (0.1 THz), or $\alpha_{\text{MGT}} = 1.32$ ($< \alpha_{\text{BCS}}$) to within errors giving the same parameters as BEMA fits. As shown in Fig. 5, the superfluid spectral weight $S_{\delta,\text{MGT}}$ extracted from MGT $G_1(\nu)$ is now just slightly below the experimental S_{δ,G_2}. This indicates that the MGT G_2 also converges to near the experimental data at frequencies lower than 0.2 THz.

These fits with effective medium models show that although there can be a low frequency absorption coming from inhomogeneity, this does not completely explain the extracted small gaps in these systems. Therefore one can take this as an intrinsic feature of the superconducting state of β-W. One possibility is that the gap is strongly anisotropic in momentum space. Although gap anisotropy in s-wave superconductors is believed to largely depend on phonon spectrum anisotropy and not on Fermi surface anisotropies [29–31], this issue has not been investigated for the strongly anisotropic Fermi surface of tungsten. Moreover, calculations taking into account

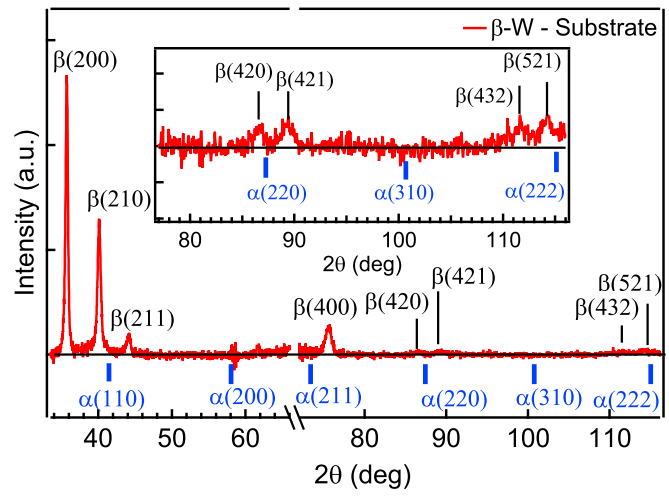

FIG. 6. $\theta - 2\theta$ x-ray diffraction pattern of tungsten thin film grown on $\text{Si}(001) + \text{SiO}_2$ substrate after subtracting the substrate intensity measured under exactly the same condition as the thin film. The β-W peaks are marked in black and the position of α-W peaks are shown with blue markers. The inset shows a zoomed-in view of diffraction intensity from 76° to 116°.

strong spin-orbit coupling in a system like tungsten with its strongly anisotropic Fermi surface [32] have not been done. This is an area for future investigation.

What is the source of these metallic regions in the film? First, we would like to discuss the possibility that the other tungsten allotrope α-W could be acting as normal metal inclusions embedded in the superconducting β-W. It is generally known that depending on the growth conditions and thickness of the thin films, tungsten grows in bcc phase, A15 phase, mixed phases, or in amorphous phase [2,3,33]. $\theta - 2\theta$ x-ray diffraction measurements on our W thin films (see Fig. 6) indicates a pure β-W phase with no α-W peaks observed within our instrumental uncertainty. We believe that α-W even if present must be much less than 10% implying that the normal volume fraction of $f = 0.3$ obtained from the effective medium models cannot be explained by normal metal inclusions of bcc W phase. Further, all the W peaks are sharp [$\beta(200)_{\mathrm{FWHM}} = 0.38^{\circ}$] indicating the absence or negligible amount of the amorphous phase [34,35]. To confirm this, we performed x-ray diffraction (XRD) measurements on W thin films grown on MgO substrate and obtained results similar to that on Si substrate (see SM [15]).

All the above, suggests that the nontrivial surface states of the topological Dirac metal of β-W [7] are a possible source for the inhomogeneity found in the effective medium models. We estimate the grain size of β-W crystals to be 23(3) nm using the Scherrer equation [4,36] (see SM [15]). This implies that the grains of β-W are nanocrystalline and the surface to volume ratio of the entire thin film is large. Thus, in the superconducting state of nanocrystalline β-W thin films, the topological surface states on the exterior of the grains would act as sources of dissipation explaining the anomalous subgap absorption observed in our films.

P.C. and N.P.A. were supported through NSF Grant No. DMR-1905519. R.B. was supported through Air Force Office of Scientific Research, Grant No. FA9550-19-1-0082. We would like to thank T. McQueen for access to his x-ray diffractometers, and E. A. Pogue for help in performing these experiments.

[1] J. W. Gibson and R. A. Hein, Phys. Rev. Lett. **12**, 688 (1964).
[2] S. Basavaiah and S. R. Pollack, J. Appl. Phys. **39**, 5548 (1968).
[3] J. Hofer and N. Haberkorn, Thin Solid Films **685**, 117 (2019).
[4] Q. Hao, W. Chen, and G. Xiao, Appl. Phys. Lett. **106**, 182403 (2015).
[5] S. Mondal, S. Choudhury, N. Jha, A. Ganguly, J. Sinha, and A. Barman, Phys. Rev. B **96**, 054414 (2017).
[6] K.-U. Demasius, T. Phung, W. Zhang, B. P. Hughes, S.-H. Yang, A. Kellock, W. Han, A. Pushp, and S. S. P. Parkin, Nat. Commun. **7**, 10644 (2016).
[7] J. Li, S. Ullah, R. Li, M. Liu, H. Cao, D. Li, Y. Li, and X.-Q. Chen, Phys. Rev. B **99**, 165110 (2019).
[8] T. Xie, M. Dreyer, D. Bowen, D. Hinkel, R. E. Butera, C. Krafft, and I. Mayergoyz, IEEE Trans. Nanotechnol. **17**, 914 (2018).
[9] A. R. Mellnik, J. S. Lee, A. Richardella, J. L. Grab, P. J. Mintun, M. H. Fischer, A. Vaezi, A. Manchon, E.-A. Kim, N. Samarth, and D. C. Ralph, Nature (London) **511**, 449 (2014).
[10] W. L. Bond, A. S. Cooper, K. Andres, G. W. Hull, T. H. Geballe, and B. T. Matthias, Phys. Rev. Lett. **15**, 260 (1965).
[11] J. Xiao, P. Liu, Y. Liang, H. B. Li, and G. W. Yang, Nanoscale **5**, 899 (2013).
[12] J. Bardeen, L. N. Cooper, and J. R. Schrieffer, Phys. Rev. **106**, 162 (1957).
[13] R. Khasanov and I. I. Mazin, Phys. Rev. B **103**, L060502 (2021).
[14] J. Carbotte, *Anisotropy Effects in Superconductors* (Springer, New York, 1977), pp. 183–212.
[15] See Supplemental Material at http://link.aps.org/supplemental/10.1103/PhysRevB.105.L060503, which includes Refs. [16–20], for details about the THz measurement, effective medium approximation, and XRD characterization.
[16] J. C. M. Garnett, Philos. Trans. R. Soc. London, Ser. A **203**, 385 (1904).
[17] X. Xi, J.-H. Park, D. Graf, G. L. Carr, and D. B. Tanner, Phys. Rev. B **87**, 184503 (2013).
[18] G. L. Carr, S. Perkowitz, and D. B. Tanner, *Infrared and Millimeter Waves* (Academic, New York, 1985), pp. 171–263.
[19] C. G. Granqvist and O. Hunderi, Phys. Rev. B **16**, 3513 (1977).
[20] A. Sihvola, J. Nanomater. **2007**, 1 (2007).
[21] P. Chauhan, F. Mahmood, D. Yue, P.-C. Xu, X. Jin, and N. P. Armitage, Phys. Rev. Lett. **122**, 017002 (2019).
[22] L. H. Palmer and M. Tinkham, Phys. Rev. **165**, 588 (1968).
[23] D. C. Mattis and J. Bardeen, Phys. Rev. **111**, 412 (1958).
[24] M. Tinkham, *Introduction to Superconductivity*, 2nd ed. (Dover, New York, 2004), p. 98.
[25] W. Zimmermann, E. Brandt, M. Bauer, E. Seider, and L. Genzel, Physica C **183**, 99 (1991).
[26] M. Dressel, Adv. Condens. Matter Phys. **2013**, 104379 (2013).
[27] D. A. G. Bruggeman, Ann. Phys. **416**, 636 (1935).
[28] D. Stroud, Phys. Rev. B **12**, 3368 (1975).
[29] A. J. Bennett, Phys. Rev. **140**, A1902 (1965).
[30] P. Tomlinson and J. Carbotte, Phys. Rev. B **13**, 4738 (1976).
[31] G. W. Crabtree, D. H. Dye, D. P. Karim, S. A. Campbell, and J. B. Ketterson, Phys. Rev. B **35**, 1728 (1987).
[32] L. Mattheiss, Phys. Rev. **139**, A1893 (1965).
[33] Y. G. Shen, Y. W. Mai, Q. C. Zhang, D. R. McKenzie, W. D. McFall, and W. E. McBride, J. Appl. Phys. **87**, 177 (2000).
[34] R. Adelfar, H. Mirzadeh, A. Ataie, and M. Malekan, J. Non-Cryst. Solids **520**, 119466 (2019).
[35] G. Abrosimova, B. Gnesin, D. Gunderov, A. Drozdenko, D. Matveev, B. Mironchuk, E. Pershina, I. Sholin, and A. Aronin, Metals **10**, 1329 (2020).
[36] A. L. Patterson, Phys. Rev. **56**, 978 (1939).